2023 62nd IEEE Conference on Decision and Control (CDC)
December 13-15, 2023. Marina Bay Sands, Singapore

Adaptive Prescribed-Time Tracking Control for Fixed-wing UAV with the Input Saturation and State Constraints

Jiayi Zheng, Shulong Zhao, Qipeng Wang, Xiangke Wang and Han Zhou

Abstract— **In this paper, we propose an adaptive prescribed-time control algorithm for the fixed-wing unmanned aerial vehicle (UAV). How to follow the desired trajectory within a predetermined time is a problem worth investigating in fixed-wing UAV tracking missions. To this end, a novel method based on time-varying state feedback and segmented neural network (SNN) is proposed, using practice prescribed-time input-to-state stable to guarantee the convergence of all signals in the prescribed time. Considering the input saturation and state constraints, we give the basis for selecting the prescribed time with different initial conditions, rather than an arbitrary one. Finally, the simulation shows that the proposed method can realize prescribed-time tracking control with input saturation, despite large initial states, and the magnitude of the control changes moderately.**

I. INTRODUCTION

The system must reach the predefined position within a prescribed time in many engineering practices, such as missile guidance and space station docking. The existing methods are mainly finite-time, fixed-time and prescribed-time stabilization to meet the time constraint. The settling time of the finite-time stabilization is related to the initial state [1]. Fixed-time stabilization has overcomed this problem, but its settling time is quite conservative [2]. Subsequently, the prescribed-time controller has been proposed [3], and it is explicitly classified into two approaches: time-based scaling and state-based scaling.

A series of time-based scaling prescribed-time control methods have been proposed [4][5]. However, the structure of those methods is complex, and there are few practical application cases. The state-based scaling approach was first proposed and developed by Song [6]. Time-varying functions are used to scale the states to achieve prescribed-time convergence for the norm-form system [7]. Further, the convergence rate is improved in [8], and prescribed-time convergence is achieved with a state observer for the canonical system [9].

It should be noted that none of the above methods considers the input saturation, which must be addressed in practical systems. A saturation function based on the gaussian error function (GEF) is introduced to develop an adaptive prescribed-time sliding mode controller [10]; a time-varying Barrier Lyapunov Function (BLF) is employed to achieve the prescribed-time tracking [11].

The control of the UAV has been a research hotspot in recent years, which is approvingly demanding in time and space when performing tasks such as coordination, formation, and siege. A prescribed-time sliding mode control strategy is proposed for quadrotor UAVs [12]. In [13], the trajectory tracking problem under the input saturation of a quadrotor is solved with a prescribed-time stability control method. With model uncertainty and external disturbances, a fixed-time prescribed performance controller is proposed for a longitudinal model of the fixed-wing UAV [14].

Although there are many studies on prescribed-time methods, how to choose the parameter of the prescribed time has yet to be been considered. The prescribed-time controller is developed for higher-order integrator systems based on Time Base Generators (TBG) [15]. However, TBG has a complex structure, which is hard to select parameters flexibly in advance.

Inspired by the aforementioned works, the main contributions include the following:

(1) Combined with the model of the fixed-wing UAV, the time-varying function and SNN, we propose a prescribed-time control method under the input saturation and state constraints. Furthermore, the theoretical analysis for determining of the parameter of the prescribed time is presented.

(2) The combination of SNN and the adaptive method tackles external disturbances and the input saturation effectively, and the prescribed-time input-to-state stability is proved by Lyapunov stability analysis, which guarantees the prescribed-time convergence of all closed-loop signals. Compared with [10][16], the proposed method can compensate disturbances in a better way, and the adoption of SNN has a better adaptability to different initial states.

(3) To our best knowledge, it is the first time that a two-segment method to select the parameter of the prescribed time is proposed. Compared with [17], the proposed method is more tolerant to the initial states and the magnitude of control changes moderately. Moreover, the selected parameter of the prescribed time is reasonable, which is verified by the simulation.

The rest of the paper is organized as follows. First, we give the necessary preliminaries in Section II. Then in Section III, we present the design and analysis of the proposed controller and the basis for selecting the parameter of the prescribed time. Section IV demonstrates our simulation results and compares them with the existing work. Finally,

This work was supported by the National Natural Science Foundation of China under Grants 6197022394 and U2241214.

Jiayi Zheng, Shulong Zhao, Qipeng Wang, Xiangke Wang and Han Zhou are with College of Intelligence Science and Technology, National University of Defense Technology, Changsha, 410000, China *(Corresponding author: Shulong Zhao)* jiayi_zheng@nudt.edu.cn, jaymaths@nudt.edu.cn, wangqipeng@nudt.edu.cn, xkwang@nudt.edu.cn

the conclusion is drawn in Section V.

Notations: Throughout this paper, as for any vector $\mathbf{x}(t) \in \mathbb{R}^n$, the norm of $\mathbf{x}(t)$ is defined as $\|\mathbf{x}(t)\| = \sqrt{x_1^2(t)+\cdots+x_n^2(t)}$ and $\mathbf{x}^2 = \mathbf{x}^T\mathbf{x}$. Besides, the term $\lambda_{min}(A)$ with $A \in \mathbb{R}^{n\times n}$ denotes the minimum eigenvalue of A, and $exp(x)$ represents e^x.

II. Preliminaries

In this section, we give the model of the fixed-wing UAV first, and some relevant definitions and lemmas are presented.

A. Model of Fixed-wing UAV

Refer to our previous work [18], the model of the fixed-wing UAV with external disturbances and unmodeled dynamics can be expressed as

$$\begin{aligned}
\dot{x} &= v cos\psi cos\gamma + w_x \\
\dot{y} &= v sin\psi cos\gamma + w_y \\
\dot{z} &= v sin\gamma + w_z \\
\dot{v} &= \frac{F}{m} \\
\dot{\psi} &= \frac{g}{v} tan\phi_c \\
\dot{\gamma} &= \tau_0(\gamma_c - \gamma),
\end{aligned} \tag{1}$$

where x, y, z represent the position of the UAV, v, ψ, γ represent the airspeed, course angle and path angle, respectively. F, ϕ_c, γ_c respectively denote the combined external force, commanded roll angle and commanded path angle as the control inputs. m, g are the mass and gravitational acceleration, and τ_0 is the time constant. w_x, w_y, w_z represent the bounded disturbances along x, y, z, with unknown boundaries of $|w_i| \le w_{im}, i = x, y, z$.

As a practical system, the fixed-wing UAV is constrained by the control inputs and the rate of states, therefore the constraints and the input saturation are introduced as follows:

$$\begin{aligned}
&|\dot{\psi}| \le \dot{\psi}_m,\ |\gamma| < \frac{\pi}{2},\ |\dot{\gamma}| \le \dot{\gamma}_m,\ \underline{v} \le v \le \bar{v},\ |\dot{v}| \le \dot{v}_m, \\
&|u_i| \le u_{im}, i = 1,2,3,
\end{aligned} \tag{2}$$

where $u_1 = \frac{F}{m},\ u_2 = \frac{g}{v} tan\phi_c,\ u_3 = \tau_0(\gamma_c - \gamma)$ represent acceleration, heading angular rate and pitch angular rate, whose maximum values are $\dot{v}_m,\ \dot{\psi}_m,\ \dot{\gamma}_m$, respectively, i.e. $u_{1m} = \dot{v}_m,\ u_{2m} = \dot{\psi}_m,\ u_{3m} = \dot{\gamma}_m$.

To restrict the control inputs in this paper, we use the following function [17]:

$$\rho(\alpha) = \iota^* tanh(\frac{\alpha}{\iota^*}) = \iota^* \frac{e^{\alpha/\iota^*} - e^{-\alpha/\iota^*}}{e^{\alpha/\iota^*} + e^{-\alpha/\iota^*}}, \tag{3}$$

where ι^* is a positive constant. Apparently, $\rho(\alpha)$ is a smooth function with the boundary of $(-\iota^*, \iota^*)$, which is differentiable at $\alpha = 0$. By the median theorem, it follows

$$\begin{aligned}
\rho(\alpha) &= \frac{\partial \rho(\bar{\alpha})}{\partial \alpha}(\alpha - \alpha_0) + \rho(\alpha_0), \\
\frac{\partial \rho(\bar{\alpha})}{\partial \alpha} &= \frac{4}{(e^{\alpha/\iota^*} + e^{-\alpha/\iota^*})^2} \le 1,
\end{aligned} \tag{4}$$

where $\bar{\alpha} \in (\alpha_0, \alpha),\ \alpha_0 < \alpha$.

For simplicity of calculation, we choose $\alpha_0 = 0$, then (4) can be expressed as

$$\rho(\alpha) = \frac{\partial \rho(\bar{\alpha})}{\partial \alpha}\alpha = \rho^* \alpha,$$

where $0 \le \rho^* \le 1$.

Denote $\mathbf{p}_1 = [x, y, z]^T,\ \tilde{\mathbf{p}}_2 = [f_x, f_y, f_z]^T,\ \mathbf{U} = [u_1, u_2, u_3]^T$, where $f_x = v cos\psi cos\gamma,\ f_y = v sin\psi cos\gamma,\ f_z = v sin\gamma,\ v = \sqrt{f_x^2 + f_y^2 + f_z^2} \in [\underline{v}, \bar{v}]$, and further $\underline{v} \le |f_i| \le \bar{v},\ i = x, y, z$. Then denote $\mathbf{p}_2 = \tilde{\mathbf{p}}_2 - [\frac{\underline{v}+\bar{v}}{2}, \frac{\underline{v}+\bar{v}}{2}, \frac{\underline{v}+\bar{v}}{2}]^T$ with $|\mathbf{p}_{2i}| \le \frac{\bar{v}-\underline{v}}{2},\ i = x, y, z$.

Thus, (1) can be simplified as:

$$\begin{aligned}
\dot{\mathbf{p}}_1 &= \mathbf{p}_2 + [\frac{\underline{v}+\bar{v}}{2}, \frac{\underline{v}+\bar{v}}{2}, \frac{\underline{v}+\bar{v}}{2}]^T + \mathbf{w}, \\
\dot{\mathbf{p}}_2 &= \mathbf{B}\mathbf{U},
\end{aligned} \tag{5}$$

where $\mathbf{w} = [w_x, w_y, w_z]^T$,

$$\mathbf{B} = \begin{bmatrix} cos\psi cos\gamma & -v sin\psi cos\gamma & -v sin\psi sin\gamma \\ sin\psi cos\gamma & v cos\psi cos\gamma & -v sin\psi sin\gamma \\ sin\gamma & 0 & v cos\gamma \end{bmatrix}.$$

From (2)(3), $\mathbf{U}$ can be expressed as $\mathbf{U} = \rho(\mathbf{U}) + \Delta\mathbf{U}$ with the boundary of $\mathbf{U}_m = [u_{1m}, u_{2m}, u_{3m}]^T$, where $\Delta\mathbf{U} = [\Delta u_1, \Delta u_2, \Delta u_3]^T$. Then we introduce the following assumption:

Assumption 1: For $i = 1, 2, 3$, assume $|\Delta u_i| \le d_i(t)\eta_i(u_i)$, where $d_i(t)$ has an unknown boundary denoted as $|d_i(t)| \le d_{im},\ t \in [t_0, t_0 + T)$, and $\eta_i(u_i) \ge 0$ is a known scalar continuous function.

Remark 1: This assumption is reasonable and can be found in [19] for reference.

B. Definitions and Lemmas

The design of the prescribed-time controller is mainly based on the following monotonically increasing time-varying function:

$$\zeta_1(t - t_0) = \frac{T}{T + t_0 - t},\ t \in [t_0, t_0 + T),$$

where $T > 0$, and $\zeta_1(0) = 1, \zeta_1(T) = +\infty$. In this paper, we choose $t_0 = 0$.

Definition 1: [6] The system $\dot{x} = f(x, t, d_w)$ is said to be PT-ISS+C in time T and converge to zero if there exist class KL functions σ and σ_f, and a class K function γ, such that, for all $t \in [t_0, t_0 + T)$,

$$|x(t)| \le \sigma_f(\sigma(|x_0|, t - t_0) + \gamma(|d_w|), \zeta_1(t - t_0) - 1).$$

Lemma 1: [6] Consider the function

$$\zeta(t - t_0) = \frac{T^{n+m}}{(T + t_0 - t)^{n+m}} = \zeta_1(t - t_0)^{n+m}, \tag{6}$$

on $t \in [t_0, t_0 + T)$, with positive integers $m,\ n$. If a continuously differentiable function $V : [t_0, t_0 + T) \to [0, +\infty)$ satisfies

$$\dot{V}(t) \le -2k\zeta(t - t_0)V(t) + \frac{\zeta(t - t_0)}{4\varpi} d_w^2(t) + \zeta(t - t_0)\Gamma,$$

for positive constants $k,\ \varpi$ and Γ, then

$$V(t) \le \mu(t - t_0)^{2k} V(t_0) + \frac{|d_w|^2}{8k\varpi} + \frac{\Gamma}{2k}, \tag{7}$$

where μ is the monotonically decreasing function

$$\mu(t-t_0) = e^{\frac{T}{m+n-1}\left(1-\zeta_1(t-t_0)^{m+n-1}\right)}, \tag{8}$$

with the properties that $\mu(0)=1$ and $\mu(T)=0$.

Lemma 2: [20] For any $\kappa>0$ and $\chi\in\mathbb{R}$, the inequality $0\le|\chi|-\chi\tanh\left(\frac{\chi}{\kappa}\right)\le\kappa_0\kappa$ holds, where κ_0 is a constant that satisfies $\kappa_0=\exp(-(\kappa_0+1))$.

C. Segmented Neural Networks

For any continuous function $f(\cdot)$ and any given constant $\varepsilon_m>0$, there exists a NN $W\phi_i(\chi)$ with enough nodes r, such that

$$f(\cdot)=W^T\phi_i(\chi)+\varepsilon,\ \|\varepsilon\|\le\varepsilon_m,$$

where $W=[W_1,W_2,\ldots,W_r]^T$ represents the ideal estimated weight parameter, and ε and $\phi_i(\chi)$ represent the estimated residual and the basis function vector, respectively. And generally the Gaussian function is used for $\phi_i(\chi)$:

$$\phi_i(\chi)=\exp\left(-\frac{(\chi-\mu_{\chi i})^T(\chi-\mu_{\chi i})}{\rho_i^2}\right), i=1,2,\ldots,r,$$

where μ_{χ_i} and ρ_i represent the center and the width of the basis function, respectively.

Within a small tight compact, NN has a relatively effective approximation, however, to match the approximation more closely to the real value. To this end, SNN is utilized [20], [21] and [22]. The following function is introduced to switch between segments.

Definition 2: Define constants $0<\xi_{i1}<\xi_{i2}$ as the boundaries of the compact subsets Ω_i, and switching functions is given as

$$m_i(\bar{\chi}_i)\triangleq\prod_{k=1}^{i}M_k(\chi_k),$$

$$M_k(\chi_k)\triangleq\begin{cases}1, & |\chi_k|<\xi_{k1}\\ \dfrac{\xi_{k2}^2-\chi_k^2}{\xi_{k2}^2-\xi_{k1}^2}e^{-\left(\frac{\chi_k^2-\xi_{k1}^2}{\lambda(\xi_{k2}^2-\xi_{k1}^2)}\right)^{2b}}, & \xi_{k1}\le|\chi_k|\le\xi_{k2}\\ 0, & |\chi_k|>\xi_{k2}\end{cases}$$

where $\bar{\chi}_i=[\chi_1,\ldots,\chi_i]^T$, and $\lambda>0,\ b\ge1$ being the spread and the order of the function $M_k(\chi_k)$, respectively.

III. Main Work

The main work is organized into the following two parts: III-A introduces the design of the prescribed-time controller, and III-B presents the basis for selecting the parameter of the prescribed time.

A. Controller Design

This section uses the backstepping method to design control and adaptive laws for (5). According to (5), $n=2$ in (6), i.e. $\zeta(t-t_0)=\zeta_1^{2+m}(t-t_0)$.

Define $\mathbf{s}_1=\zeta(\mathbf{p}_1-\mathbf{p}_r),\ \mathbf{s}_2=\zeta(\mathbf{p}_2-\rho(\alpha_1))$, where α_1 is the virtual controller with the boundary of $\iota_1^*=\frac{\bar{\nu}-\nu}{2}$. The desired trajectory is denoted as $\mathbf{p}_r=[x_r,y_r,z_r]^T$ with $|\dot{p}_{ri}|\le\dot{p}_{rim}$.

Remark 2: From [23], we can know that there exist positive constants $\bar{b},\ \underline{b}$ such that $\underline{b}\le\lambda_{min}((\mathbf{B}+\mathbf{B}^T)/2)$. This is the basis for $\underline{b}$ in *Theorem* 1.

Theorem 1: Consider the fixed-wing UAV (1), in which the unknown input saturation is estimated by SNN, and the adaptive controller $\alpha_1,\ \mathbf{U},\ \hat{\theta}_i,\ \hat{H}_i$ are given by:

$$\alpha_1=-\frac{2+m}{T}\mathbf{s}_1-k_1\mathbf{s}_1-m_1u_1^s-(1-m_1)u_1^c, \tag{9}$$

$$\mathbf{U}=\frac{1}{\underline{b}}\left[-\frac{\mathbf{s}_1}{\zeta}-\frac{2+m}{T}\mathbf{s}_2-k_2\mathbf{s}_2-\varpi\vartheta^2\mathbf{s}_2-m_2u_2^s-(1-m_2)u_2^c\right], \tag{10}$$

$$u_i^s=\mathbf{s}_i^T\hat{\theta}_i\phi_i^T\phi_i,\ u_i^c=\mathbf{s}_i^T\hat{H}_i tanh(\frac{\mathbf{s}_i^2}{\kappa_i}),$$

$$\dot{\hat{\theta}}_i=\mathbf{s}_i^2\zeta m_i\phi_i^T\phi_i-\zeta\hat{\theta}_i, \tag{11}$$

$$\dot{\hat{H}}_i=\mathbf{s}_i^2\zeta(1-m_i)tanh(\frac{\mathbf{s}_i^2}{\kappa_i})-\zeta\hat{H}_i,\ i=1,2, \tag{12}$$

where $\kappa_i>0,\ \vartheta=[\eta_1,\eta_2,\eta_3]^T,\ u_i^s,\ u_i^c$ represent the SNN controller and the convergent controller, respectively, and $\hat{\theta}_i$ is the estimation of $\theta_i=W_i^TW_i$, $\hat{H}_i$ is the estimation of H_i. H_i, k_i will be defined later.

Based on (9)(10), the following conclusions can be obtained within $t\in[t_0,t_0+T)$: (1) The system (1) can track the desired trajectory and achieve the practical prescribed-time convergence. (2) With the time-varying state feedback, the controller can ensure that all signals are remained bounded.

Proof: **Step 1:** The derivative of $\mathbf{s}_1$ gives:

$$\begin{aligned}\dot{\mathbf{s}}_1&=\dot{\zeta}(\mathbf{p}_1-\mathbf{p}_r)+\zeta\mathbf{p}_2+\zeta[\iota_1^*,\iota_1^*,\iota_1^*]^T+\zeta\mathbf{w}-\zeta\dot{\mathbf{p}}_r\\&=\dot{\zeta}(\mathbf{p}_1-\mathbf{p}_r)+\mathbf{s}_2+\zeta\rho(\alpha_1)+\zeta\mathbf{h}_1,\end{aligned} \tag{13}$$

where $\mathbf{h}_1=[\iota_1^*,\iota_1^*,\iota_1^*]^T+\mathbf{w}-\dot{\mathbf{p}}_r$. Since $\mathbf{w}$ is a bounded disturbance and $\dot{\mathbf{p}}_r$ has a known boundary, $\mathbf{h}_1$ can be estimated by

$$\zeta\mathbf{h}_1=\zeta\left(W_1^T\phi_1+\varepsilon_1\right),\|\mathbf{h}_1\|\le\|[\iota_1^*,\iota_1^*,\iota_1^*]^T+\mathbf{w}_m+\dot{\mathbf{p}}_{rm}\|=H_1, \tag{14}$$

where H_1 is the upper boundary of $\|\mathbf{h}_1\|$, which is unknown but can be estimated by SNN.

Substituting (14) into (13), we have

$$\begin{aligned}\dot{\mathbf{s}}_1=&\dot{\zeta}(\mathbf{p}_1-\mathbf{p}_r)+\mathbf{s}_2+\zeta\rho(\alpha_1)+\zeta m_1\left(W_1^T\phi_1+\varepsilon_1\right)\\&+\zeta(1-m_1)\mathbf{h}_1.\end{aligned}$$

Choose Lyapunov function as $V_1=\frac{1}{2}\mathbf{s}_1^2+\frac{1}{2}\tilde{\theta}_1^2+\frac{1}{2}\tilde{H}_1^2$, derivation of V_1 gives:

$$\begin{aligned}\dot{V}_1=&\mathbf{s}_1^T\dot{\mathbf{s}}_1+\tilde{\theta}_1^T\dot{\tilde{\theta}}_1+\tilde{H}_1^T\dot{\tilde{H}}_1\\=&\mathbf{s}_1^T\dot{\zeta}(\mathbf{p}_1-\mathbf{p}_r)+\mathbf{s}_1^T\mathbf{s}_2+\mathbf{s}_1^T\zeta\rho(\alpha_1)+\mathbf{s}_1^T\zeta(1-m_1)\mathbf{h}_1\\&+\mathbf{s}_1^T\zeta m_1\left(W_1^T\phi_1+\varepsilon_1\right)-\tilde{\theta}_1^T\dot{\hat{\theta}}_1-\tilde{H}_1^T\dot{\hat{H}}_1,\end{aligned} \tag{15}$$

where $\tilde{\theta}_1=\theta_1-\hat{\theta}_1,\ \tilde{H}_1=H_1-\hat{H}_1$.

For (15), the following inequalities are obtained by Young's inequality:

$$\mathbf{s}_1^T\dot{\zeta}(\mathbf{p}_1-\mathbf{p}_r)\le \mathbf{s}_1^T\zeta\frac{2+m}{T}\rho^*\zeta(\mathbf{p}_1-\mathbf{p}_r)=\mathbf{s}_1^2\zeta\frac{2+m}{T}\rho^*,$$
$$\mathbf{s}_1^T\zeta m_1\left(W_1^T\phi_1+\varepsilon_1\right)\le\frac{\zeta m_1}{4\rho^*}+\zeta m_1\mathbf{s}_1^2\rho^*\theta_1\phi_1^T\phi_1+\mathbf{s}_1^T\zeta m_1\varepsilon_1,$$
$$\mathbf{s}_1^T\zeta(1-m_1)\mathbf{h}_1\le\frac{\zeta(1-m_1)H_1}{4\rho^*}+\zeta(1-m_1)\mathbf{s}_1^2\rho^*H_1,$$
$$\mathbf{s}_1^T\zeta\rho(\alpha_1)\le\mathbf{s}_1^T\zeta\rho^*\alpha_1,$$

where ρ^* is chosen as:

$$\rho^*=\begin{cases}1, & t=t_0\\ \rho_0\in[\zeta_1^{-(1+m)},1]. & t\in(t_0,T)\end{cases}$$

According to Lemma 2, we have

$$\zeta(1-m_1)\rho^*H_1\left(\mathbf{s}_1^2-\mathbf{s}_1^2tanh(\frac{\mathbf{s}_1^2}{\kappa_1})\right)\le\zeta(1-m_1)\rho^*H_1\kappa_0\kappa_1.$$

Thus (15) can be reduced to

$$\dot{V}_1\le\mathbf{s}_1^T\mathbf{s}_2-\mathbf{s}_1^2\zeta\rho^*k_1+\mathbf{s}_1^T\zeta m_1\varepsilon_1+\zeta\tilde{\theta}_1^T\hat{\theta}_1+\zeta\tilde{H}_1^T\hat{H}_1+\zeta(1-m_1)\rho^*H_1\kappa_0\kappa_1+\frac{\zeta m_1}{4\rho^*}+\frac{\zeta(1-m_1)H_1}{4\rho^*}.$$

Step 2: Derivation for $\mathbf{s}_2$ yields:

$$\begin{aligned}\dot{\mathbf{s}}_2&=\dot{\zeta}(\mathbf{p}_2-\rho(\alpha_1))+\zeta(\mathbf{B}\mathbf{U}-\dot{\alpha}_1)\\&=\dot{\zeta}(\mathbf{p}_2-\rho(\alpha_1))+\zeta\mathbf{B}\mathbf{U}+\zeta\mathbf{h}_2,\end{aligned}\tag{16}$$

where $\mathbf{h}_2=-\dot{\alpha}_1$.

Remark 3: Here $\dot{\alpha}_1=\frac{\partial\alpha_1}{\mathbf{s}_1}\dot{\mathbf{s}}_1+\frac{\partial\alpha_1}{\hat{\theta}_1}\dot{\hat{\theta}}_1+\frac{\partial\alpha_1}{\hat{H}_1}\dot{\hat{H}}_1$, which is bounded. The similar conclusion can be found in [23].

Since $\dot{\alpha}_1$ is bounded and $\frac{\partial\rho(\alpha_1)}{\partial\alpha_1}$ has the boundary of 1, $\mathbf{h}_2$ can be estimated by

$$\zeta\mathbf{h}_2=\zeta\left(W_2^T\phi_2+\varepsilon_2\right),\ \|\mathbf{h}_2\|\le H_2,\tag{17}$$

where H_2 is the upper bound of $\|\mathbf{h}_2\|$, which is unknown but can be estimated by SNN.

Substituting (17) into (16), we get

$$\dot{\mathbf{s}}_2=\dot{\zeta}(\mathbf{p}_2-\rho(\alpha_1))+\zeta\mathbf{B}\rho(\mathbf{U})+\zeta\mathbf{B}\Delta\mathbf{U}+\zeta m_2\left(W_2^T\phi_2+\varepsilon_2\right)+\zeta(1-m_2)\mathbf{h}_2,$$

where $\iota_2^*=U_m=\|\mathbf{U}_m\|$.

Choose Lyapunov function $V_2=\frac{1}{2}\mathbf{s}_2^2+\frac{1}{2}\tilde{\theta}_2^2+\frac{1}{2}\tilde{H}_2^2$, where $\tilde{\theta}_2=\theta_2-\hat{\theta}_2,\ \tilde{H}_2=H_2-\hat{H}_2$. Similar to **Step 1**, combined with the following inequality:

$$\mathbf{s}_2^T\zeta\mathbf{B}\Delta\mathbf{U}\le\mathbf{s}_2^T\zeta\mathbf{B}d(t)\vartheta(u)\le\mathbf{s}_2^2\zeta\varpi\vartheta^2+\frac{\zeta}{4\varpi}(\mathbf{B}d)^2,$$

where $\varpi>0$. The derivative of V_2 gives

$$\dot{V}_2\le-\mathbf{s}_2^T\rho^*\mathbf{s}_1-\mathbf{s}_2^2\zeta\rho^*k_2+\frac{\zeta}{4\varpi}(\mathbf{B}d)^2+\frac{\zeta m_2}{4\rho^*}+\mathbf{s}_2^T\zeta m_2\varepsilon_2+\frac{\zeta(1-m_2)H_2}{4\rho^*}+\zeta\tilde{\theta}_2^T\hat{\theta}_2+\zeta\tilde{H}_2^T\hat{H}_2+\zeta(1-m_2)\rho^*H_2\kappa_0\kappa_2.$$

Choose $V=V_1+V_2$, and derivation for V yields:

$$\begin{aligned}\dot{V}&=\dot{V}_1+\dot{V}_2\\&\le\sum_{i=1}^{2}\Big(-\zeta\rho^*k_i\mathbf{s}_i^2+\zeta\tilde{\theta}_i^T\hat{\theta}_i+\zeta\tilde{H}_i^T\hat{H}_i+\mathbf{s}_i^T\zeta m_i\varepsilon_i+\frac{\zeta m_i}{4\rho^*}+\frac{\zeta(1-m_i)H_i}{4\rho^*}1+\zeta(1-m_i)\rho^*H_i\kappa_0\kappa_i\Big)+(1-\rho^*)\mathbf{s}_1^T\mathbf{s}_2+\frac{\zeta}{4\varpi}(\mathbf{B}d)^2.\end{aligned}$$

According to Young's inequality, we have

$$\begin{aligned}(1-\rho^*)\mathbf{s}_1^T\mathbf{s}_2&\le(1-\rho^*)\left|\mathbf{s}_1^T\mathbf{s}_2\right|\\&\le\frac{1}{2}\zeta(1-\rho^*)\mathbf{s}_1^2+\frac{1}{2}\zeta(1-\rho^*)\mathbf{s}_2^2\\\zeta\tilde{\theta}_i^T\hat{\theta}_i&\le\frac{1}{2}\zeta|\theta_i|^2-\frac{1}{2}\zeta|\tilde{\theta}_i|^2\\\zeta\tilde{H}_i^T\hat{H}_i&\le\frac{1}{2}\zeta|H_i|^2-\frac{1}{2}\zeta|\tilde{H}_i|^2\\\mathbf{s}_i^T\zeta m_i\varepsilon_i&\le\frac{1}{2}\zeta\mathbf{s}_i^2+\frac{1}{2}\zeta\varepsilon_{im}^2,\end{aligned}$$

where $i=1,2$. Thus

$$\dot{V}\le-2k\zeta V+\frac{\zeta}{4\varpi}(\mathbf{B}d)^2+\zeta\Gamma,\tag{18}$$

where $k=\frac{1}{2}\min\{\rho^*k_1+\frac{1}{2}\rho^*-1,\rho^*k_2+\frac{1}{2}\rho^*-1,1\}$ with $k_1,k_2>\frac{2-\rho^*}{2\rho^*}$ and $\Gamma=\sum_{i=1}^{2}\Big(\frac{1}{2}|\theta_i|^2+\frac{1}{2}|H_i|^2+\frac{1}{2}\varepsilon_{im}^2+\frac{m_i}{4\rho^*}+\frac{(1-m_i)H_i}{4\rho^*+(1-m_i)\rho^*H_i\kappa_0\kappa_i}\Big)$. Here the proof is completed. ■

B. Selection of the Prescribed Time T_p

The parameter of prescribed time is organized in two segments, as shown in Fig 1. o is a small neighborhood near the origin, which indicates the practical prescribed-time convergence; ξ_p is the region of initial states that can be tolerated based on the practical situation. The initial states in $[\mathrm{o},\xi_p]$ can be unified by the state-scaling function to the boundary ξ_p. In other words, calculating the prescribed time of the boundary ξ_p can guarantee the prescribed-time convergence of the initial states in $[\mathrm{o},\xi_p]$.

Under the input saturation, T_1 is the time of converging to o when the initial state is within ξ_p, and T_2 is the time of convergence from an arbitrary position to ξ_p. Therefore, the total convergence time T with any initial states is the combination of these two segments, i.e.

$$T=T_1+aT_2,\ a=\begin{cases}0, & s_i\in[\mathrm{o},\xi_p]\\ 1, & s_i\in[\xi_p,+\infty)\end{cases},$$

where $i=1,2$.

1) T_1: In the first segment, $\xi_{p1}=\|\mathbf{s}_1\|=\|\zeta(\mathbf{p}_{p1}-\mathbf{p}_r)\|,\ \xi_{p2}=\|\mathbf{s}_2\|=\|\zeta(\mathbf{p}_{p2}-\rho(\alpha_1))\|$.

From (9)(10), we have:

$$\|\alpha_1\|\le\left|\frac{2+m}{T}+k_1+\underline{k}_1\right|\|\mathbf{s}_1\|=\left(\frac{2+m}{T}+k_1+\underline{k}_1\right)\xi_{p1},$$
$$\|\mathbf{U}\|\le\frac{\|\mathbf{s}_1\|}{\underline{b}}+\frac{1}{\underline{b}}\left|\frac{2+m}{T}+k_2+\varpi\vartheta^2+\underline{k}_2\right|\|\mathbf{s}_2\|=\frac{1}{\underline{b}}\xi_{p1}+\frac{1}{\underline{b}}\left(\frac{2+m}{T}+k_2+\varpi\vartheta^2+\underline{k}_2\right)\xi_{p2},$$

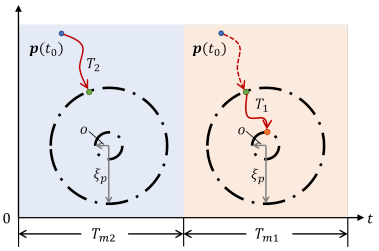

Fig. 1. Two segments of prescribed-time convergence.

where $\varphi_i = \phi_i^T \phi_i$ is a fixed value, and $tanh(\frac{\mathbf{s}_i^2}{\kappa_i}) \leq \frac{\pi}{2}$, $\underline{k}_i = m_i\hat{\theta}_i\varphi_i + (1-m_i)\hat{H}_i\frac{\pi}{2} > 0$, $i = 1,2$.

The boundary of the controller α_1 and $\mathbf{U}$ are $\iota_1^* = \frac{\bar{v}-\underline{v}}{2}$, $\iota_2^* = U_m$, respectively. To make the controller satisfy the constraint, then

$$\left(\frac{2+m}{T} + k_1 + \underline{k}_1\right)\xi_{p1} \leq \frac{\bar{v}-\underline{v}}{2},$$
$$\frac{1}{\underline{b}}\xi_{p1} + \frac{1}{\underline{b}}\left(\frac{2+m}{T} + k_2 + \varpi\vartheta^2 + \underline{k}_2\right)\xi_{p2} \leq U_m, \tag{19}$$

Solving the above inequalities yields

$$T_1 \geq T_{m1} = max\{T_{m11}, T_{m12}\}, \tag{20}$$

where $T_{m11} = \frac{2\xi_{p1}(2+m)}{\bar{v}-\underline{v}-2\xi_{p1}(k_1+\underline{k}_1)}$, and $T_{m12} = \frac{\xi_{p2}(2+m)}{\underline{b}U_m - \xi_{p1} - \xi_{p2}(\varpi\vartheta^2+k_2+\underline{k}_2)}$.

2) T_2: In the second segment, $\xi_{\delta 1} = \|\mathbf{s}_1\| - \xi_{p1} = \|\zeta(\mathbf{p}_1 - \bar{\mathbf{p}}_r)\|$, $\xi_{\delta 2} = \|\mathbf{s}_2\| - \xi_{p2} = \|\zeta(\mathbf{p}_2 - \bar{\rho}(\alpha_1))\|$, where $\bar{\mathbf{p}}_r = \mathbf{p}_r - \mathbf{p}_{p1}$, $\bar{\rho}(\alpha_1) = \rho(\alpha_1) - \mathbf{p}_{p2}$.

According to (9)(10)(18), we have

$$\|\alpha_1\| \leq \left(\frac{2+m}{T} + k_1 + \underline{k}_1\right)\xi_{\delta 1},$$
$$\|\mathbf{U}\| \leq \frac{1}{\underline{b}}\xi_{\delta 1} + \frac{1}{\underline{b}}\left(\frac{2+m}{T} + k_2 + \varpi\vartheta^2 + \underline{k}_2\right)\xi_{\delta 2},$$
$$\dot{V} \leq -2k\zeta V + \frac{\zeta}{4\varpi}(\mathbf{B}d)^2 + \zeta\Gamma,$$

and combined with (7)(8), we have

$$\frac{1}{2}\mathbf{s}_1^2 + \frac{1}{2}\mathbf{s}_2^2 \leq V \leq \mu(t-t_0)^{2k}V(t_0) + \frac{\|\mathbf{B}d\|^2}{8k\varpi} + \frac{\Gamma}{2k} \leq \frac{1}{2}\Xi^2,$$

where $\Xi = \sqrt{2V(t_0) + \frac{\|\mathbf{B}d\|^2}{4k\varpi} + \frac{\Gamma}{k}}$. Then we have $\|\mathbf{s}_1\| \leq \Xi$, $\|\mathbf{s}_2\| \leq \Xi$, i.e.

$$\xi_{\delta 1} \leq \Xi - \xi_{p1}, \xi_{\delta 2} \leq \Xi - \xi_{p2}.$$

In a similar way to (19), we can obtain

$$T_2 \geq T_{m2} = max\{T_{m21}, T_{m22}\}, \tag{21}$$

where $T_{m21} = \frac{2(\Xi-\xi_{p1})(2+m)}{\bar{v}-\underline{v}-2(\Xi-\xi_{p1})(k_1+\underline{k}_1)}$, $T_{m22} = \frac{(\Xi-\xi_{p2})(2+m)}{\underline{b}U_m - (\Xi-\xi_{p1}) - (\Xi-\xi_{p2})(\varpi\vartheta^2+k_2+\underline{k}_2)}$.

Combine (20) and (21), and select the parameter of the prescribed time as follows

$$T_p = T_{m1} + T_{m2} = max\{T_{m11} + T_{m21}, T_{m12} + T_{m22}\}.$$

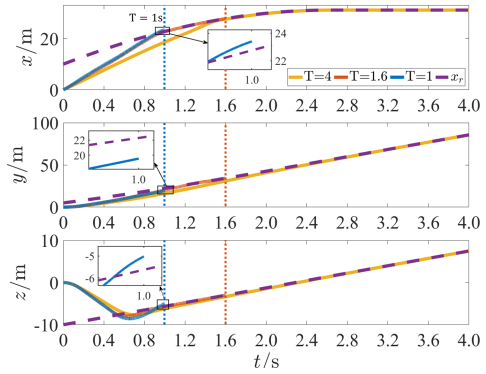

Fig. 2. Tracking performance under different prescribed time T.

IV. Simulation

In this section, we perform the following simulations: in section IV-A, the basis for selecting of the time is verified, and in section IV-B, we compare the tracking performance of our work with [17].

Some of the parameters in the simulation are set as follows: $m = 1$, $\bar{v} = 34$, $\underline{v} = 20$, $\iota_1^* = 27$, $\iota_2^* = 100$. The initial state of the fixed-wing UAV is $x(1) = y(1) = z(1) = 0$, $v(1) = 20$, $\psi(1) = 0$, $\gamma(1) = 0$. Moreover, assume a virtual fixed-wing UAV with initial state of $x_r = 10$, $y_r = 5$, $z_r = -10$, $v_r = 22$, $\psi_r = \pi/4$, $\gamma_r = 0.2$ and $a_r = 0$, $\dot{\psi}_r = 0.3$, $\dot{\gamma}_r = 0$, whose trajectory is considered as the desired. All simulations are realized under Matlab R2020b.

A. Selection of T_p

Firstly, $s_{p1} = 55$, $s_{p2} = 5$ is chosen to obtain $T_{m1} = 1.6s$ based on (20).

To verify the result in III-B, we choose three prescribed times $T = 1s$, $T = 1.6s$ and $T = 4s$, as shown in Fig 2. It is evident that under the input saturation, the controller cannot track the desired trajectory when $T = 1s$, which indicates that the prescribed time cannot be chosen arbitrarily. When $T = 1.6s$, the system tracks the desired trajectory precisely, and when $T = 4s$, the system has already tracked the desired trajectory at $t = 2.2s$, thus the choice of $T = 4s$ loses the advantage of the prescribed-time method.

B. Comparison with the Exiting Method

Based on IV-A, we choose $T = 2s$ as the paremeter of the prescribed time in this section. A comparison between the methods of us and [6] is demonstrated in Fig 3. The initial states of [6] are the same as the proposed's.

Remark 4: In the method of [6], the convergence problem is considered, but the simulation reveals that the method of [6] does not converge under some specific initial states. To have a better comparison, the following transformations are done for states $\mathbf{p}_1$, $\mathbf{p}_2$ while calculating the control inputs: $\bar{\mathbf{p}}_1 = \mathbf{p}_1 - \mathbf{p}_{1r}$, $\bar{\mathbf{p}}_2 = \mathbf{p}_2 - \mathbf{p}_{2r}$. Therefore, in Fig.3, the method [6] has the opposite convergence direction of x, y, z compared to the proposed.

It can be seen that:

(1) Both methods can track the time-varying trajectory at the prescribed time. However, it is obvious that the proposed method converges faster and has higher convergence

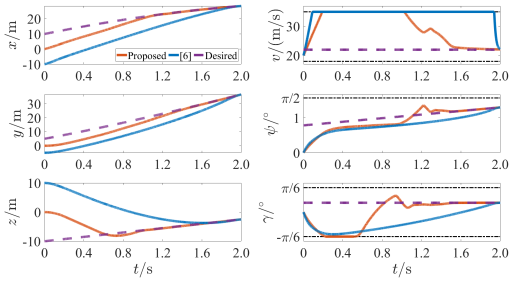

(a) States of the fixed-wing UAV.

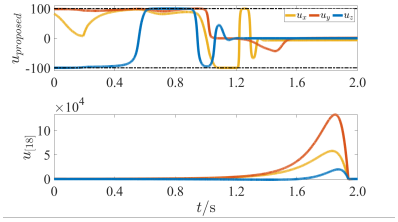

(b) Magnitude of the control.

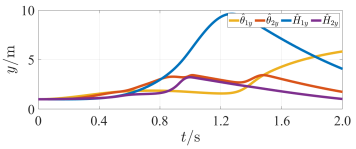

(c) The SNN estimation.

Fig. 3. Tracking performance compared with [6], $T = 2s$.

accuracy. In addition, the proposed method uses a lesser order of the time-varying function than that in [6], which is less computationally intensive and suitable for onboard computation. Therefore, in the case of large initial states, the proposed method performs better and is more applicable to the practical fixed-wing UAV.

(2) The proposed method can achieve the prescribed-time tracking with moderate control changes under the input saturation, while the input of the method proposed in [6] being enormous (almost 13×10^4), which is not allowed in the practical system.

V. Conclusions

In this paper, an adaptive prescribed-time control based on the time-varying function and SNN is presented for the fixed-wing UAV, and the basis for selecting the parameter of the prescribed time of the controller is presented. SNN is used to estimate the unknown parameters, and PT-ISS+C is used to deal with unknown disturbances conveniently, which guarantee the prescribed-time convergence of all closed-loop signals simultaneously. The simulations show the advantages of the proposed method, through comparing with the existing method, including high tolerance for initial states and moderate changes of the magnitude of the control. In addition, selecting the parameter of the prescribed time avoids unreasonable configuration in advance.

References

[1] A. Polyakov and A. Poznyak, "Lyapunov function design for finite-time convergence analysis: "twisting" controller for second-order sliding mode realization," *Automatica*, vol. 45, no. 2, pp. 444–448, 2009.

[2] A. Polyakov, "Nonlinear feedback design for fixed-time stabilization of linear control systems," *IEEE Transactions on Automatic Control*, vol. 57, no. 8, pp. 2106–2110, 2012.

[3] A. K. Pal, S. Kamal, S. K. Nagar, B. Bandyopadhyay, and L. Fridman, "Design of controllers with arbitrary convergence time," *Automatica*, vol. 112, p. 108710, 2020.

[4] P. Krishnamurthy, F. Khorrami, and M. Krstic, "A dynamic high-gain design for prescribed-time regulation of nonlinear systems," *Automatica*, vol. 115, p. 108860, 2020.

[5] P. Krishnamurthy, F. Khorrami and M. Krstic, "Robust adaptive prescribed-time stabilization via output feedback for uncertain nonlinear strict-feedback-like systems," *European Journal of Control*, vol. 55, pp. 14–23, 2020.

[6] Y. Song, Y. Wang, J. Holloway, and M. Krstic, "Time-varying feedback for regulation of normal-form nonlinear systems in prescribed finite time," *Automatica*, vol. 83, no. C, p. 243–251, sep 2017.

[7] Y. Song, Y. Wang, and M. Krstic, "Time-varying feedback for stabilization in prescribed finite time," *International Journal of Robust and Nonlinear Control*, vol. 29, no. 3, pp. 618–633, 2019.

[8] Y. Wang and Y. Song, "A general approach to precise tracking of nonlinear systems subject to non-vanishing uncertainties," *Automatica*, vol. 106, pp. 306–314, 2019.

[9] J. Holloway and M. Krstic, "Prescribed-time observers for linear systems in observer canonical form," *IEEE Transactions on Automatic Control*, vol. 64, no. 9, pp. 3905–3912, 2019.

[10] Z. Gao, Y. Zhang, and G. Guo, "Fixed-time prescribed performance adaptive fixed-time sliding mode control for vehicular platoons with actuator saturation," *IEEE Transactions on Intelligent Transportation Systems*, vol. 23, no. 12, pp. 24 176–24 189, 2022.

[11] R. Ma, L. Fu, and J. Fu, "Prescribed-time tracking control for nonlinear systems with guaranteed performance," *Automatica*, vol. 146, p. 110573, 2022.

[12] S. Zhou, K. Guo, X. Yu, L. Guo, and L. Xie, "Fixed-time observer based safety control for a quadrotor uav," *IEEE Transactions on Aerospace and Electronic Systems*, vol. 57, no. 5, pp. 2815–2825, 2021.

[13] B. Zhu, M. Chen, and T. Li, "Prescribed performance–based tracking control for quadrotor uav under input delays and input saturations." *Transactions of the Institute of Measurement & Control*, vol. 44, no. 10, pp. 2049 – 2062, 2022.

[14] J. Tan and S. Guo, "Backstepping control with fixed-time prescribed performance for fixed wing uav under model uncertainties and external disturbances," *International Journal of Control*, 2020.

[15] H. M. Becerra, C. R. Vázquez, G. Arechavaleta, and J. Delfin, "Predefined-time convergence control for high-order integrator systems using time base generators," *IEEE Transactions on Control Systems Technology*, vol. 26, no. 5, pp. 1866–1873, 2018.

[16] H. Ye and Y. Song, "Robust adaptive prescribed-time control for parameter-varying nonlinear systems," *ArXiv*, vol. abs/2210.12706, 2022.

[17] Z. Liu, C. Lin, and Y. Shang, "Prescribed-time adaptive neural feedback control for a class of nonlinear systems," *Neurocomputing*, pp. 155–162, 2022.

[18] S. Zhao, X. Wang, Z. Lin, D. Zhang, and L. Shen, "Integrating vector field approach and input-to-state stability curved path following for unmanned aerial vehicles," *IEEE Transactions on Systems, Man, and Cybernetics: Systems*, vol. 50, no. 8, pp. 2897–2904, 2020.

[19] J. Su and Y. Song, "Prescribed-time control under unknown control gain and mismatched nonparametric uncertainties," *Systems & Control Letters*, vol. 171, p. 105420, 01 2023.

[20] B. Xu, C. Yang, and Y. Pan, "Global neural dynamic surface tracking control of strict-feedback systems with application to hypersonic flight vehicle," *IEEE Transactions on Neural Networks and Learning Systems*, vol. 26, no. 10, pp. 2563–2575, 2015.

[21] J.-T. Huang, "Global tracking control of strict-feedback systems using neural networks," *IEEE Transactions on Neural Networks and Learning Systems*, vol. 23, no. 11, pp. 1714–1725, 2012.

[22] C. Zhu, Y. Jiang, and C. Yang, "Fixed-time neural control of robot manipulator with global stability and guaranteed transient performance," *IEEE Transactions on Industrial Electronics*, vol. 70, no. 1, pp. 803–812, 2023.

[23] H. Ye and Y. Song, "Prescribed-time tracking control of mimo nonlinear systems under non-vanishing uncertainties," *IEEE Transactions on Automatic Control*, pp. 1–8, 2022.